Soils and Rocks
An International Journal of Geotechnical and Geoenvironmental Engineering
www.soilsandrocks.com
ISSN 1980-9743
ISSN-e 2675-5475

Undrained shear strength degradation and consolidation coefficients evaluation considering a piezoball penetrometer: application on a Brazilian soft soil deposit

Jonatas Sosnoski[1#], Gracieli Dienstmann[1], André Luis Meier[1], Edgar Odebrecht[2], Helena Paula Nierwinski[1]

Article

Keywords
In situ testing
Site investigation
Geotechnical engineering
Piezoball
Piezocone

Abstract

This study presents the application of a piezoball penetrometer equipped with pore pressure transducers at the tip, mid-face, and equator positions to characterize the undrained shear strength and consolidation behavior of a soft clay deposit in southern Brazil. Two piezoball tests were performed with cyclic and dissipation measurements, alongside piezocone, field vane, and laboratory tests. Undrained strength estimates based on penetration resistance aligned well with piezocone and vane test results, using an average bearing factor aligned with international practice. Remolded strength revealed sensitivity to the time interval between penetration and extraction readings, with longer delays leading to overestimation. Dissipation tests showed contractive pore pressure behavior, and consolidation coefficients derived from normalized curves at the equator sensor position were closest to piezocone-based values. The study provides practical recommendations for piezoball testing and highlights the importance of time control during cyclic measurements, reinforcing the importance of expanding robust geotechnical databases to support future applications.

1. Introduction

The growing demand for in-situ assessment of undrained shear strength has driven the development of penetration testing methods, particularly for offshore engineering applications (Liu et al., 2023). In this context, flow penetrometer tests have evolved largely in response to the limitations associated with traditional field vane tests and piezocone penetration tests (CPTu) in accurately determining continuous profiles of undrained shear strength (O'Loughlin et al., 2020, Qiao et al., 2023). In fact, the field vane test is widely recognized as one of the most reliable methods for determining undrained shear strength and soil sensitivity under simple shear conditions (Schnaid, 2009). Its main drawback, however, is that it provides only localized point measurements, thereby limiting its applicability for continuous profiling.

CPTu testing has become standard practice for obtaining continuous profiles of penetration resistance and pore pressure response, allowing the assessment of soil stratigraphy and drainage conditions with depth (Lunne et al., 1997; Robertson, 2009). Nevertheless, a major challenge associated with CPTu interpretation lies in the selection of appropriate bearing capacity factors required to convert cone resistance measurements into undrained shear strength, as these factors are influenced by soil type, stress history, and drainage conditions during penetration (Schnaid, 2009; Mayne, 2007; Robertson, 2009).

Flow penetrometer tests consist of advancing a probe equipped with either a ball or a T-bar tip while continuously measuring penetration resistance. These devices promote a full-flow soil mechanism around the probe, under which the conversion factors used to derive undrained shear strength—namely the bearing capacity factors N_b for ball penetrometers and N_t for T-bar penetrometers—are expected to be less sensitive to local soil characteristics and stress history (DeJong et al., 2011; Colreavy et al., 2012).

An advancement of this technology, the piezoball, and piezo-T, integrates pore pressure transducers at different positions such as at the probe's tip (u_1), mid-face (u_2), and equator (u_3) positions, which enables dissipation tests to be performed at predetermined depths for the determination of permeability and consolidation parameters. The location of the transducers plays a critical role in selecting the most appropriate theoretical framework for data interpretation. Theoretical (Mahmoodzadeh et al., 2015; Liu et al., 2023) and empirical approaches (Colreavy et al., 2016) are available

#Corresponding author. E-mail address: jonatas.sosnoski@gmail.com
[1]Universidade Federal de Santa Catarina, Programa de Pós-graduação em Engenharia Civil, Florianópolis, SC, Brasil.
[2]Universidade do Estado de Santa Catarina, Programa de Pós-graduação em Engenharia Civil, Joinville, SC, Brasil.

Submitted on June 1, 2025; Final Acceptance on January 30, 2026; Discussion open until November 30, 2026.
Editor: Renato P. Cunha
https://doi.org/10.28927/SR.2026.008625

in the literature and should be interpreted considering the transducer positions assessed by the respective authors.

Another advantage of using the piezoball and Piezo-T penetrometer is their ability to assess clay remolded strength (S_{ur}) behavior and sensitivity (S_T). This parameter can be determined by directly comparing the undrained shear strength profiles obtained during initial penetration with those measured after performing cyclic penetration and extraction at predefined depths (e.g., Yafrate & DeJong, 2007). Furthermore, monitoring the extraction resistance of the probe offers insights into the degree of soil disturbance. In this context, Yafrate et al. (2009) proposed a method to estimate remolded strength without the need for cyclic loading, which could potentially reduce testing time and associated costs.

The application of ball-type penetrometer tests (piezoball) remains limited in Brazil. This study introduces the first Brazilian piezoball device, developed by Meert (2022) and Sosnoski (2024), and applied during a site investigation campaign on a soft clay deposit in Tubarão, Santa Catarina State. The experimental results were systematically compared with data from piezocone penetration tests, laboratory vane shear tests, and laboratory analyses. This comprehensive comparison provides valuable insights into the applicability, performance, and potential advantages of the piezoball approach for soft clay characterization.

2. Theoretical background

The use of piezoball penetrometer tests is not recent and has been reported by several authors over the years, who highlight its advantages over piezocone tests, especially regarding the accuracy in determining undrained shear strength (e.g., Yafrate et al., 2009; Colreavy et al., 2010; Mahmoodzadeh et al., 2015). Furthermore, studies by Low et al. (2007) and Colreavy et al. (2015) indicated that normalized dissipation times in piezoball tests are shorter than those observed in piezocone tests, offering a practical advantage.

The measured penetration resistance (q_m) during piezoball testing results primarily from soil flow around the ball and is influenced by the geostatic stress acting on the probe. To correct for the effects of the unequal areas at the top and base of the equipment, the cross-sectional area of the probe (A_p) and the area of the pushing rod immediately above the ball (A_s) were considered by Randolph (2004) for determining the net strength (q_{net}), as expressed in Equation 1.

$$q_{net} = q_m - \left[\sigma_{v0} - u\left(1-a\right)\right]\frac{A_s}{A_p} \tag{1}$$

where σ_{v0} is the total stress, u denotes the hydrostatic pore pressure, and parameter a is the ratio of equipment load cell areas. Recommendations in the literature suggest the use of equipment with an area ratio (A_R=A_p/A_s), of approximately 10:1 (Yafrate et al., 2009; Lunne et al., 2011). However, experimental results indicate that ratios greater than 5:1 are generally sufficient to minimize the influence of the pushing rod on the soil flow mechanism around the probe and, consequently, on the measurement of q_m.

The piezoball test can also be employed to perform cyclic testing, which involves repeated insertion and extraction of the probe at predetermined depths while monitoring the mobilized resistances throughout the cycles. The results of these cycling processes can be used to investigate soil strength degradation mechanisms (DeJong et al., 2010).

Some recommendations regarding the execution of cyclic tests can be outlined as follows: a minimum displacement range of 150 mm, or at least three times the ball diameter, is suggested to ensure adequate soil remolding; stabilization of the mobilized resistance is typically achieved after approximately ten cycles (Chung & Randolph, 2004; Yafrate & DeJong, 2005; Lunne et al., 2011; Yubin et al., 2019); cyclic loading should be initiated immediately after the probe reaches the target depth to minimize the effects of potential soil consolidation, which may influence the results (DeJong et al., 2010).

During cyclic testing, the monitoring of strength degradation can be performed by determining the remolded penetration strength (q_{rem}), which is defined as the average of the penetration (q_{in}) and extraction (q_{ext}) resistances measured after the tenth cycle or upon reaching stabilization. The remolded penetration strength (q_{rem}) can then be applied in theoretical strain-softening models, such as the one proposed by Einav & Randolph (2005), to predict strength degradation as a function of the number of cycles. In a more recent approach, Yafrate et al. (2009) presented Equation 2 to predict the strength of a given cycle (q_n) based on the number of cycles (n) and the number of cycles required to reach 95% of strength degradation (N_{95}):

$$\frac{q\left(n\right)}{q_{in}} = \frac{q_{rem}}{q_{in}} + \left(1 - \frac{q_{rem}}{q_{in}}\right)e^{-3\left(n-0.5\right)/N_{95}} \tag{2}$$

where q_n is the strength of a given cycle, q_{in} is the strength for the initial penetration, and q_{rem} is the remolded strength. For the application of this approach, the value of N_{95}, which represents the number of cycles required to achieve 95% of the total strength degradation, is determined based on the experimentally measured initial (q_{in}) and remolded (q_{rem}) penetration resistances.

Yafrate et al. (2009) also proposed an empirical relationship to predict the remolded strength (q_{rem}) based on the extraction resistance (q_{ext}) when cyclic tests are not performed, as shown in Equation 3. Furthermore, the authors suggested that N_{95}, could also be estimated directly from the extraction measurements using Equation 4, which was derived from Equation 3, leading to the generalized expression presented in Equation 5.

$$\frac{q_{rem}}{q_{in}} = \left(\frac{q_{ext}}{q_{in}}\right)^{2.8} \tag{3}$$

$$N_{95} = 9.6\left(\frac{q_{ext}}{q_{in}}\right) \tag{4}$$

$$\frac{q(n)}{q_{in}} = \left(\frac{q_{ext}}{q_{in}}\right)^{2.8}\left(\frac{q_{ext}}{q_{in}}\left(\frac{q_{ext}}{q_{in}}\right)^{2.8}\right)e^{-\frac{3(n-1)}{9.6\left(\frac{q_{ext}}{q_{in}}\right)}} \tag{5}$$

The mobilized resistances (q_{net}) are used to estimate the undrained shear strength (S_u), which can be determined from the ratio between the net penetration resistance (q_{net}) and a bearing capacity factor (N_b), as expressed in Equation 6.

$$S_u = \frac{q_{net}}{N_b} \tag{6}$$

where N_b is a bearing capacity factor that depends on the roughness of the spherical probe, characterized by the roughness factor (α).

The theoretical solution of Randolph (2004) indicates that the roughness factor can vary from 0 (perfectly smooth) to 1 (rough), outlining values of N_b between 10.97 and 15.31, respectively. Although this solution presents a considerable variation in the values of N_b, Chung & Randolph (2004) recommended adopting a representative value N_b of 10.5 for flow penetrometers, which produced consistent estimates of *Su* in field applications when compared to values obtained from the field vane test (FVT). Clay sensitivity can be directly determined using FVT data as shown in Equation 7. Additionally, Yafrate et al. (2009), based on data from five testing sites, proposed empirical correlations for estimating S_T from piezoball test results by relating the ratios q_{in}/q_{rem} and $q_{in}/_{ext}$ presented in Equations 8 and 9, respectively:

$$S_T = \frac{S_u}{S_{ur}} \tag{7}$$

$$S_T = \left(\frac{q_{in}}{q_{rem}}\right)^{1.4} \tag{8}$$

$$S_T = \left(\frac{q_{in}}{q_{ext}}\right)^{3.7} \tag{9}$$

DeJong et al. (2011) advise that the primary soil property that influences values of N_b is sensitivity (S_T), presented in Equation 7, and suggested the estimation of the resistance factor from this parameter according to Equation 10. Based on Yafrate et al. (2009) proposal, the authors also suggest an equation based on q_{in}/q_{ext} (equation 11) for estimating sensitivity.

DeJong et al. (2011) stated that the primary soil property influencing the bearing capacity factor N_b is the sensitivity (S_T), defined in Equation 7. Furthermore, the authors proposed an empirical correlation to estimate N_b as a function of S_T, as presented in Equation 10. Building upon the approach of Yafrate et al. (2009), DeJong et al. (2011) also suggested an alternative expression to estimate soil sensitivity based on the ratio q_{in}/q_{ext} provided in Equation 11.

$$N_b = 13.2 - \frac{7.5}{1+\left(\frac{S_T}{10}\right)^{-3}} \tag{10}$$

$$N_b = 13.2 - \frac{7.5}{1+\left(\frac{q_{in}/q_{ext}}{1.9}\right)^{-20}} \tag{11}$$

For the estimation of the undrained remolded shear strength S_{ur} a specific factor N_{rem}, distinct from N_b must be considered (Equation 12). Yafrate et al. (2009) proposed a relationship to estimate N_{rem} based on the soil sensitivity (S_T) presented in Equation 13. In cases where sensitivity is not directly determined N_{rem} can alternatively be estimated using the penetration-to-extraction ratio, due to the empirical correlation between this ratio and soil sensitivity, as expressed in Equation 14.

$$S_{ur} = \frac{q_{rem}}{N_{rem}} \tag{12}$$

$$N_{rem} = 13.2 + \frac{7.5}{1+\left(\frac{S_T}{8}\right)^{-3}} \tag{13}$$

$$N_{rem} = 13.2 + \frac{7.5}{1+\left(\frac{q_{in}/q_{ext}}{1.8}\right)^{-20}} \tag{14}$$

In a more practical approach, the correction factors can be directly determined through calibration against field vane test results or undrained shear strength values obtained from laboratory triaxial tests (DeJong et al., 2010).

The piezoball dissipation test can be used to evaluate the hydraulic conductivity and the coefficient of consolidation of soft soils (Low et al., 2007; DeJong et al., 2008). For such tests, it is recommended that at least 50% of the generated excess pore pressure dissipates (DeJong et al., 2010), regardless of the position of the penetrometer's pore pressure transducer. In this context, Kelleher & Randolph (2005) and Colreavy et al. (2010) used devices capable of measuring pore pressures at the equator (u_3) and the mid-face (u_2) of the penetrometer. DeJong et al. (2008) presented equipment capable of measuring at these two locations as well as at the tip of the ball (u_1). There is still no consensus regarding the optimal sensor position for interpreting the excess pore pressure dissipation in the piezoball test; however, some studies (e.g., Colreavy et al., 2016; Mahmoodzadeh et al., 2015) have reported consistent results for estimating the horizontal coefficient of consolidation (c_h) using readings at u_2. In the present study, a piezoball equipped with three sensor positions is considered.

For dissipation test interpretation, the normalized excess pore pressure $\Delta u/\Delta u_{ini}$ evolution with a normalized time T can be analyzed, where Δu represents the excess pore pressure at a given time and Δu_{ini} is the initial excess pore pressure. The normalized dissipation time, T, follows the classical formulation proposed by Teh & Houlsby (1991) (Equation 15), from which c_h can be determined according to Equation 16:

$$T = \frac{c_h\, t}{D^2\, I_r^{0.5}} \tag{15}$$

$$c_h = \frac{T_{50} D_c^2 I_r^{0.5}}{t_{50}} \tag{16}$$

where t_{50} is the time required for 50% dissipation of the excess pore pressure generated, D_c is the diameter of the piezocone, and I_r is the rigidity index of the soil, with a T_{50} of 0.245.

Inspired by the classical solution proposed by Teh & Houlsby (1991), Mahmoodzadeh et al. (2015) (Equation 17) and Liu et al. (2023) (Equation 18) presented similar approaches for establishing a unique dissipation curve in the $\Delta u/\Delta u_{ini} - T_b$, space, where T_b represents the normalized time specific to the piezoball test.

$$\frac{\Delta u}{\Delta u_{ini}} \approx \frac{1}{1+\dfrac{T_b}{T_{b50}}} \quad with \quad T_{b50} = \frac{c_h t_{50}}{D_b d I_r^{0,25}} \tag{17}$$

$$\frac{\Delta u}{\Delta u_{ini}} \approx \frac{1}{\left(1+\dfrac{T_b}{T_{b50}}\right)^{0.9}} \quad with \quad T_{b50}\,\frac{c_h t_{50}}{\left(\dfrac{D_b}{2}\right)^2 I_r^{0,25}} \tag{18}$$

where T_{b50} is the dimensionless time for 50% of dissipation to occur, with values of 0.12 and 0.18 for the positions u_2 and u_3 according to the proposal by Mahmoodzadeh et al. (2015) and 0.44 for the position u_3 according to Liu et al. (2023).

Equation 19 is proposed for estimating c_h through the dissipation of piezoball based on the normalization proposed by Mahmoodzadeh et al. (2015):

$$c_h = \frac{T_{b50} D_b d I_r^{0,25}}{t_{50}} \tag{19}$$

where D_b and d are the ball's and pushing rod's diameters just above the ball, respectively.

Liu et al. (2023) also proposed an alternative approach for estimating c_h based on readings at position u_3 (Equation 20):

$$c_h = \frac{T_{b50}\left(\dfrac{D_b}{2}\right)^2 I_r^{0,25}}{t_{50}} \tag{20}$$

Colreavy et al. (2016) elaborated an empirical proposal for estimating c_h from readings taken at the equator position (u_3). In this case, a value of t_{max} is used, which indicates the time required to reach the highest value of excess pore pressure generated in the dissipation test, in addition to the dissipation time of 50% ($t_{50\%}$) according to Equation 21:

$$c_h = 0.7\left(\frac{D_b d I_r^{0,25}}{t_{max}}\right)\left(\frac{t_{max}}{t_{50}}\right)^{1.2} \tag{21}$$

3. Materials and methods

This study was carried out at an experimental site in Tubarão, Santa Catarina State, Brazil (Figure 1). The area is part of a Quaternary lagoon system and is characterized by very soft, normally consolidated clays overlain by thin sandy–silty layers (Odebrecht & Schnaid, 2018). These soils present high compressibility, elevated water content, and low shear strength.

3.1 Characterization campaign

To ensure result consistency, an initial testing campaign—hereafter referred to as the "conventional campaign" — was carried out. The tests were conducted following an investigation grid layout with 1.5 m spacing between test points. The conventional campaign included piezocone tests, vane shear tests, and the collection of undisturbed samples for laboratory characterization, consolidation, and triaxial testing. Additionally, piezocone dissipation tests were performed at reference depths of 4.8, 6.8, and 7.8 m. Undisturbed samples were collected at depths of 4, 5, 7, 8, 9, and 10 m. A summary of the testing campaign is presented in Table 1 and 2.

The soils are predominantly silty (MH, PI ≈ 35%), with specific gravity around 2.7, high initial void ratios (e_0 = 2.6–3.6), and high compressibility (C_c = 1.1–2.7). Table 1 presents a summary of the parameters obtained from characterization and consolidation tests, including a quality assessment of the samples based on the criteria proposed by Lunne et al. (1997) and Coutinho (2007). Notably, samples retrieved at greater depths exhibited lower quality ratings. Nevertheless, the plasticity and compressibility parameters are generally consistent with the expected range for Brazilian soft clays (Schnaid, 2009; Baroni, 2010; Dienstmann et al., 2021).

Isotropically Consolidated Undrained Triaxial Compression (CIU) tests were performed on samples retrieved at depths of 8, 9, and 10 m. At each depth, three specimens were tested under confining stresses (σ_c) of 25, 50, and 100 kPa. Table 2 presents a basic compilation of the results. Strength parameters were interpreted at maximum axial strain to reduce dependence on the initial sample structure. Results revealed low effective cohesion values (approximately 2 kPa) and effective friction angles ranging from 20.9° to 25.4°, which are consistent with normally consolidated clays of similar geological and physical characteristics.

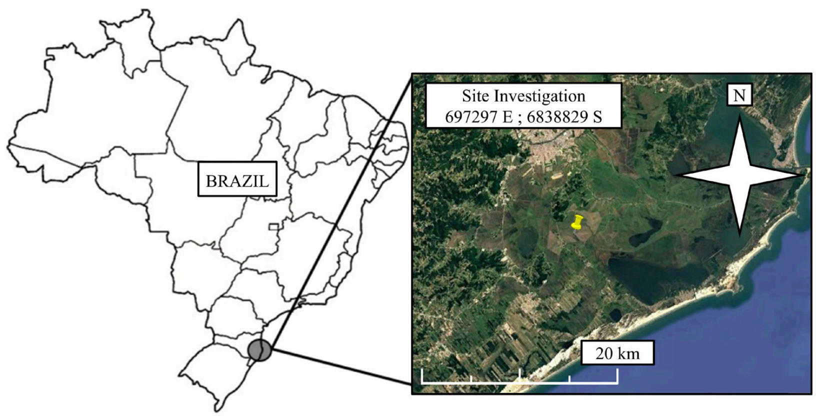

Figure 1. Location of investigation site.

Table 1. Tubarão soil properties: characterization and oedometer tests.

Depth (m)	*LL* (%)	*LP* (%)	*IP* (%)	*G*	γ (kN/m³)	e_0	*w* (%)	c_v (cm²/s)	C_c	C_r	*OCR*	Lunne et al. (1997)	Coutinho (2007)
4	81.0	45.9	35.1	2.69	13.20	3.548	123.2	2.75e-4 to 1.36e-2	2.73	0.23	1.03	P	GF
5	65.0	38.5	26.5	2.70	14.04	2.732	94.3	1.12e-4 to 2.05e-3	1.48	0.17	1.02	P	P
7	67.4	29.2	38.2	2.77	13.35	3.620	124.9	1.71e-4 to 9.71e-3	2.06	0.55	1.05	GF	GF
8	65.3	30.5	34.8	2.76	14.60	2.769	103.8	1.80e-4 to 9.72e-3	1.13	0.10	0.76	P	P
9	65.4	32.8	32.6	2.78	14.00	3.080	111.6	8.5e-3 to 2.87e-2	1.44	0.14	0.82	VP	VP
10	64.3	39.4	24.9	2.71	13.89	3.238	118.0	1.3e-4 to 3.77e-2	1.31	0.16	0.68	VP	VP

P = poor; GF = good to fair; VP = very poor.

Table 2. Tubarão soil properties: triaxial tests.

Depth (m)	σ_c * (kPa)	γ (kN/m³)	e_0	*w* (%)	*c*' (kPa)	φ' (°)
8	25	14.33	2.909	107.5	1.75	25.39
	50	14.25	2.908	106.2		
	100	14.29	2.992	111.2		
9	25	14.88	2.604	98.6	2.5	23.93
	50	14.08	3.046	110.9		
	100	14.68	2.724	102.5		
10	25	14.08	3.281	122.7	2.15	20.9
	50	13.61	3.514	120.7		
	100	13.751	3.388	119.1		

*Confining stress.

Piezocone and vane test results are presented in Figure 2, comprising tip penetration resistance (q_t), pore pressure (u_2), Soil Index (IC_{rw}) behavior from Robertson & Wride (1998), undrained (S_u) and remolded (S_{ur}) shear strength values with depth, and over consolidated ratio (*OCR*). Results reveal that the site is composed of soils with clay behavior with low values of tip strength (q_t from 10 to 400 kPa) and pore pressure generation (u_2 from 0 to 230 kPa), combined with values of Ic_{RW} in the range of 3.6, corresponding to clay and organic clays as proposed by Robertson & Wride (1998). Undrained shear strength (S_u) from vane test increases along depth from 3 to 12 kPa, these values were used to define a N_{Kt}, cone correction factor, of 15.5, to determine the S_u profile in Figure 2c. Figure. 2c also displays the remolded shear strength obtained through vane test that can be used to define a sensitivity (S_T) ranging from 1.5 to 4.2 along the depth. Additionally, Figure 2d shows OCR values interpreted according to Chen & Mayne (1996), which are close to unity below 2 m depth, indicating a predominantly normally consolidated soil profile. This behavior is consistent with the low undrained shear strength values and suggests a soft, highly compressible clay deposit, which is in accordance with the oedometer test results.

3.2 Piezoball equipment

Motivated by the need for greater accuracy in predicting undrained shear strength in clayey profiles, as well as in characterizing the degradation behavior of undrained strength, flow penetrometers piezoball and piezo-T were developed through a collaboration between Geoforma Engenharia Ltda., Universidade do Estado de Santa Catarina (UDESC), and Universidade Federal de Santa Catarina (UFSC), resulting in the studies of Meert (2022) and Sosnoski (2024). This paper introduces the first Brazilian piezoball device and demonstrates its application potential through a series of tests conducted in a soft clay deposit located in Tubarão, southern Brazil. The results are interpreted in light of the available international literature, enabling an assessment of the applicability of existing interpretation frameworks and highlighting aspects that may require further refinement.

The piezoball probe developed is illustrated in Figure 3. It has an 80 mm diameter (50 cm^2 cross-sectional area, area ratio 7:1) and is fitted with three pore pressure sensors at the tip (u_1), mid-face (u_2), and equator (u_3). The penetration and extraction forces are measured by a load cell positioned immediately behind the probe, which is equipped with four strain gauges and protected by an O-ring sealing system. The load cell and the pore pressure sensors were calibrated in accordance with the recommendations of ASTM D5778 (ASTM, 2020). Further design details can be seen in Sosnoski (2024).

3.2.1 Testing program

Guidelines for the execution of ball and T-bar penetration tests, as well as basic definitions related to equipment geometry, are provided in ISO 19901-8 (ISO, 2023) and in the classical studies reviewed in Section 2, which guided the development of these devices (e.g. DeJong et al., 2010; Randolph et al., 1998). In general, the procedures adopted for full-flow penetrometer testing are similar to those used for piezocone (CPTu) testing. Accordingly, the same reaction system and rod assembly employed in CPTu testing were used, and a standard penetration rate of 20 ± 5 mm/s was adopted, with data acquisition at each second.

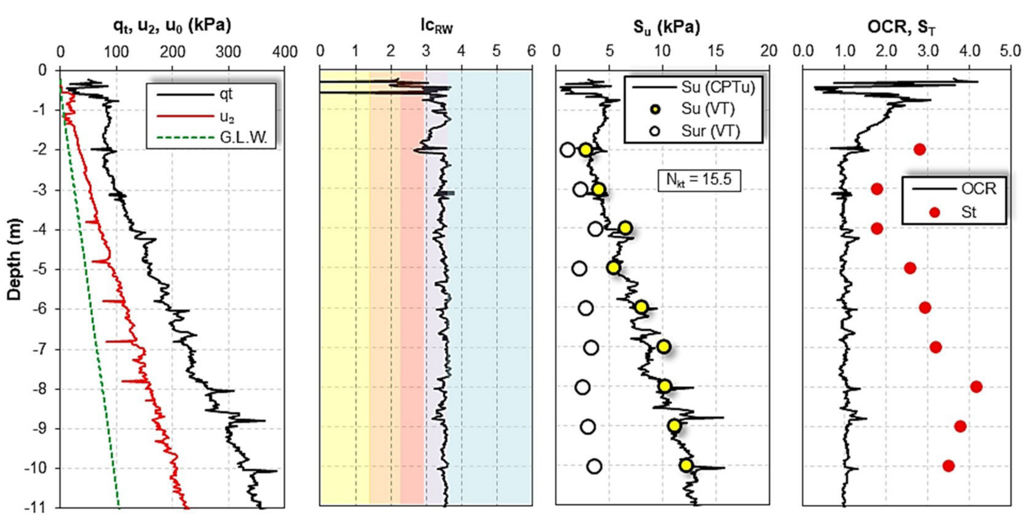

(a) (b) (c) (d)

Figure 2. General profile of conventional tests (a) CPTu tip resistance q_t, pore pressure u_2 and hydrostatic pore pressure u_{equil}; (b) Soil Index (*ICrw*) behavior from Robertson & Wride (1998); (c) undrained shear strength S_u; and (d) overconsolidation ratio *OCR* and sensibility S_T.

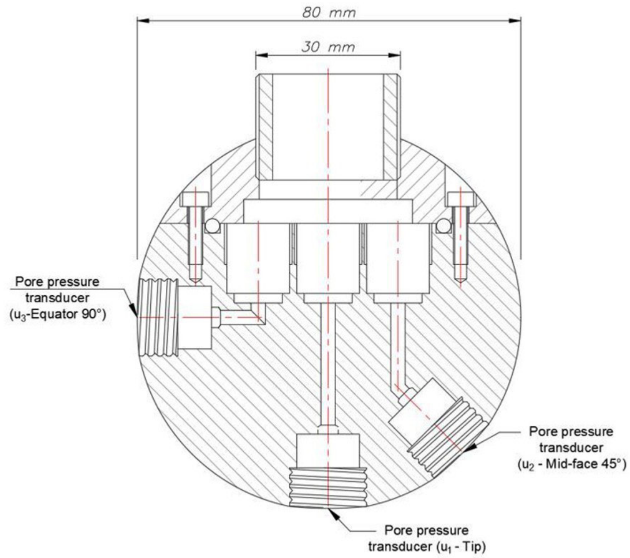

(a)

(b)

Figure 3. Piezoball penetrometer overview (a) conceptual project and (b) piezoball and 10cm² piezocone.

Table 3. Summary of cyclic and dissipation tests.

Average depth (m)	Nominal interval cycled (m)	Number of cycles		Dissipation time (s)
		Test A	Test B	Test B
-4.0	3.8 - 4.2	16	16	33160*
-6.0	5.8 - 6.2	11	14	6870
-8.0	7.8 - 8.2	14	15	6860
-10.0	9.8 - 10.2	14	16	5900

*The test at 4.0 m was performed up to 85% dissipation – however, only the reading of u_1 was recorded

During probe advancement, the forces required for penetration are measured, together with the penetration resistance (q_m) and pore pressure readings at different locations (u_1, u_2, and u_3). The measured penetration resistance may subsequently be corrected to obtain the net penetration resistance (q_{net}), as defined in Equation (1). When extraction measurements were performed, the same standard penetration rate and data acquisition frequency were adopted, in accordance with ISO 19901-8 (2023).

To evaluate the remoulded undrained shear strength, cyclic penetration tests were conducted. The adopted cycling procedure consisted of repeated insertion and extraction of the probe over minimum up-and-down distances of at least 0.15 m, or three times the ball diameter, whichever was greater. In this study, a cycle length of 0.40 m was adopted, at a nominal rate of 20 mm/s. During cyclic testing, strength degradation was monitored through the determination of the remoulded penetration resistance (q_{rem}), defined as the average of the penetration resistance (q_{in}) and extraction resistance (q_{ext}) measured after the tenth cycle or once stabilization of resistance was achieved.

Based on the observations discussed above, two piezoball tests (A and B) were performed near the characterization campaign site (described in section 3.1), with penetration at 20 mm/s. Cyclic loading was carried out at depths of 4, 6, 8, and 10 m using ranges of five ball diameters (40cm) and at least ten cycles. Test A included only cyclic loading, and the extraction resistance was measured after the total penetration of the probe. Test B incorporated dissipation tests at each target depth before cycling, with dissipation monitored at u_1, u_2, and u_3 until at least 70% pore pressure dissipation was reached. A summary of procedures is provided in Table 3.

4. Results and interpretation

Figure 4 compares the net penetration resistance (q_{net}) and pore pressure (u) obtained from Tests A and B with piezocone data. For the piezocone, q_{net} was calculated using Equation 1, with correction for vertical effective stress (σ'_{v0}), following DeJong et al. (2010).

Regarding the results shown in Figure 4, both piezoball tests showed consistent q_{net} profiles, generally lower than the

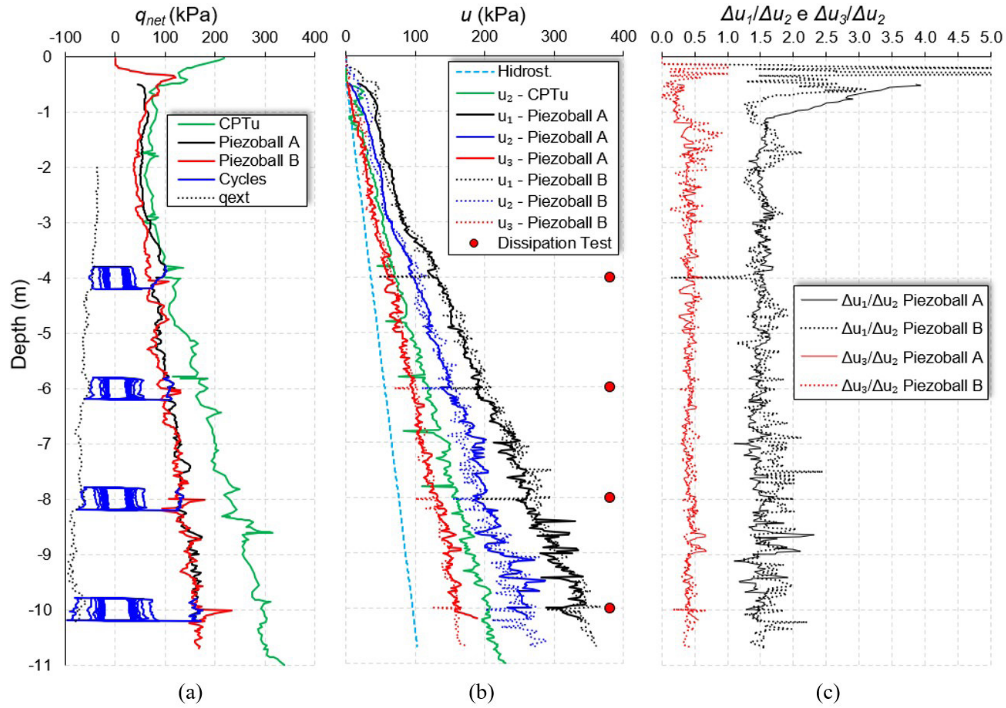

Figure 4. Results of piezoball tests (A and B) and piezocone test: (a) net penetration resistance (q_{net}); (b) pore pressure measurements; and (c) pore pressure ratios between transducer positions.

piezocone. Pore pressure measurements from the three piezoball transducers are also presented, alongside the corresponding reading from the piezocone (u_2) for reference. Overall, the measurements obtained in Tests A and B demonstrated good agreement across all transducer positions. As expected, the highest excess pore pressures were recorded at the tip transducer (u_1), intermediate values at the middle face (u_2), and the lowest values at the equator (u_3). This distribution is consistent with findings reported by Mahmoodzadeh et al. (2015) and Colreavy et al. (2016), who noted that the elevated pore pressures at the tip are associated with concentrated compressive stresses. Pore pressures measured at the middle face (u_2) were slightly higher than those recorded by the piezocone shoulder transducer (u_2–CPTu), corroborating results from centrifuge studies by Mahmoodzadeh & Randolph (2014) and Colreavy et al. (2015, 2016). Figure 4(c) shows the ratio of excess pore pressures measured at the tip (Δu_1) and equator (Δu_3) relative to the middle face (Δu_2). Except in the upper 2 meters, the $\Delta u_1/\Delta u_2$ ratio ranged between 1.3 and 1.8, while the $\Delta u_3/\Delta u_2$ ratio remained close to 0.5 in both tests. These results align closely with the values reported by Colreavy et al. (2015, 2016) for normally consolidated soils, where average $\Delta u_3/\Delta u_2$ values of 0.5 and $\Delta u_1/\Delta u_2$ values between 1.3 and 1.7 were observed.

The remolded condition of the soil was assessed through cyclic loading tests conducted at four depths (Figure 4a). For all analyses involving cyclic tests, data corresponding to displacements within one ball diameter (8.0 cm) at both ends of the cycle were excluded to minimize potential boundary effects on the results.

The results presented in Figure 4a indicate that Tests A and B exhibited similar behavior, converging to comparable remolded strength values at all tested depths. This consistency suggests good repeatability between the tests. In Test B, following dissipation, an increase in penetration resistance was observed, with q_{ext} values for the first extraction cycle (cycle 1.0) consistently higher than Test A at all depths. To apply the predictive model for remolded strength (q_{rem}) proposed by Yafrate et al. (2009), four scenarios were considered:

(i) General case: q_{ext}/q_{in} ratios calculated using the first penetration and extraction of each cycle with a fixed time gap (Δt) of 30 seconds between readings – applied only to Test A;
(ii) Continuous extraction measurement: q_{ext}/q_{in} calculated from continuous extraction data, with Δt varying by depth (e.g., 1410 s at 10 m, over 4700 s at 4 m) — also applied only to Test A;
(iii) Dissipation prior to cycling, using pre-dissipation q_{in}: q_{in} was recorded before the dissipation test, and q_{ext} after dissipation — applied to Test B. Time intervals varied with the consolidation response;
(iv) Dissipation prior to cycling, using post-dissipation q_{in}: both q_{in} and q_{ext} were recorded after dissipation — also

applied to Test B, with Δt depending on the consolidation behavior

Scenarios (iii) and (iv) aimed to investigate the effects of consolidation on remolded strength.

Results (Figure 5) show that Yafrate et al.'s (2009) model predicts q_{rem} more accurately when the time interval between q_{in} and q_{ext} readings is short ($\Delta t \approx 30$ s). Longer intervals reduce the model's predictive accuracy, likely due to partial reconsolidation or thixotropic effects (DeJong et al., 2010). This highlights the importance of minimizing delay between penetration and extraction, especially in soft soils like Tubarão's, to avoid overestimating strength recovery. When dissipation tests precede cycling (hypothesis iii and iv), the altered soil structure and drainage effects may lead to misleading q_{rem} estimates. Therefore, extraction-based analyses are best conducted in monotonic tests without prior dissipation to ensure reliability. On the other hand, tests involving continuous (monotonic) extraction also deviated from the predicted trend, with the deviation being more pronounced at shallower penetration depths. This behavior can be partially attributed to the increased time interval between penetration and extraction recorded at these depths, which may have allowed partial reconsolidation or thixotropic effects to develop in the soil structure. Additionally, the relaxation of confinement conditions near the ground surface may have contributed to changes in stress redistribution around the probe, further influencing the mobilized resistance measurements.

Figure 6 presents the results of the cyclic piezoball tests. The figure includes: (a) the degradation of the measured penetration resistance per cycle (q_n); (b) normalization of q_n by the initial penetration resistance (q_{in}) to isolate depth effects and highlight the degradation trend; and (*c*) the predicted degradation according to the model proposed by Yafrate et al. (2009).

The results in Figure 6a indicate that, for all depths and both tests, a slight reduction in q_n continues even after the 10 cycles. This residual degradation is approximately 0.6 kPa per cycle across all depths. Figure 6b shows that the normalized q_n/q_{in} values exhibit a consistent trend between Tests A and B, allowing the application of a single exponential trend line with an R^2 of 0.9282 and an overall degradation ratio (q_n/q_{in}) of approximately 0.15 after 10 cycles. The q_n/q_{in} value for the first extraction cycle tends to approach 0.50. This relationship was employed in Figure 6c to apply Yafrate et al.'s (2009) predictive model. Despite some scatter, the predicted degradation shows good agreement with the measured cyclic data from both flow penetrometers when using a q_{ext}/q_{in} ratio of approximately 0.53.

The determination of undrained shear strength (S_u) and remolded undrained shear strength (S_{ur}) was based on the direct measurements of penetration resistance (q_{net}), corrected using appropriate bearing capacity factors, N_b and N_{rem}, respectively. To estimate these factors, multiple approaches were considered: direct calibration using field vane test (FVT) results, as well as predictive methods proposed by DeJong et al. (2011) (Equations 10 and 11) and Yafrate et al. (2009) (Equations 13 and 14). Equations 10 and 13 require prior determination of soil sensitivity (ST), which in this study was derived from FVT data, with S_T values ranging from 1.5 to 4.2 (see Figure 2 and Table 4).

Predictions of S_T using the method by Yafrate et al. (2009) proved inadequate, generally yielding sensitivity values approximately six times higher than those obtained from vane tests. Therefore, preference was given to the FVT-derived values. In contrast, Equations 11 and 14 are based on the extraction ratio (q_{in}/q_{ext}), with values calculated according to the four hypotheses (i to iv).

Figure 7 presents the strength factors (N_b and N_{rem}) along depth, as well as the corresponding undrained shear strength values, S_u and S_{ur}, respectively. For N_b, values derived from field vane tests (FVT) using Equation 6 range from 12.82 to 13.16, with a mean of 12.98. When applying

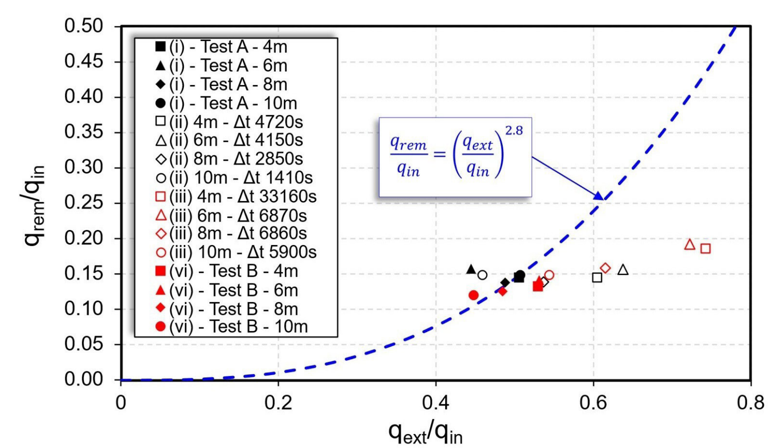

Figure 5. Relationship between extraction ratio q_{ext}/q_{in}) and normalized remolded resistance (q_{rem}/q_{in}) (Δt is defined as the time delay between q_{in} and q_{ext} measurements.

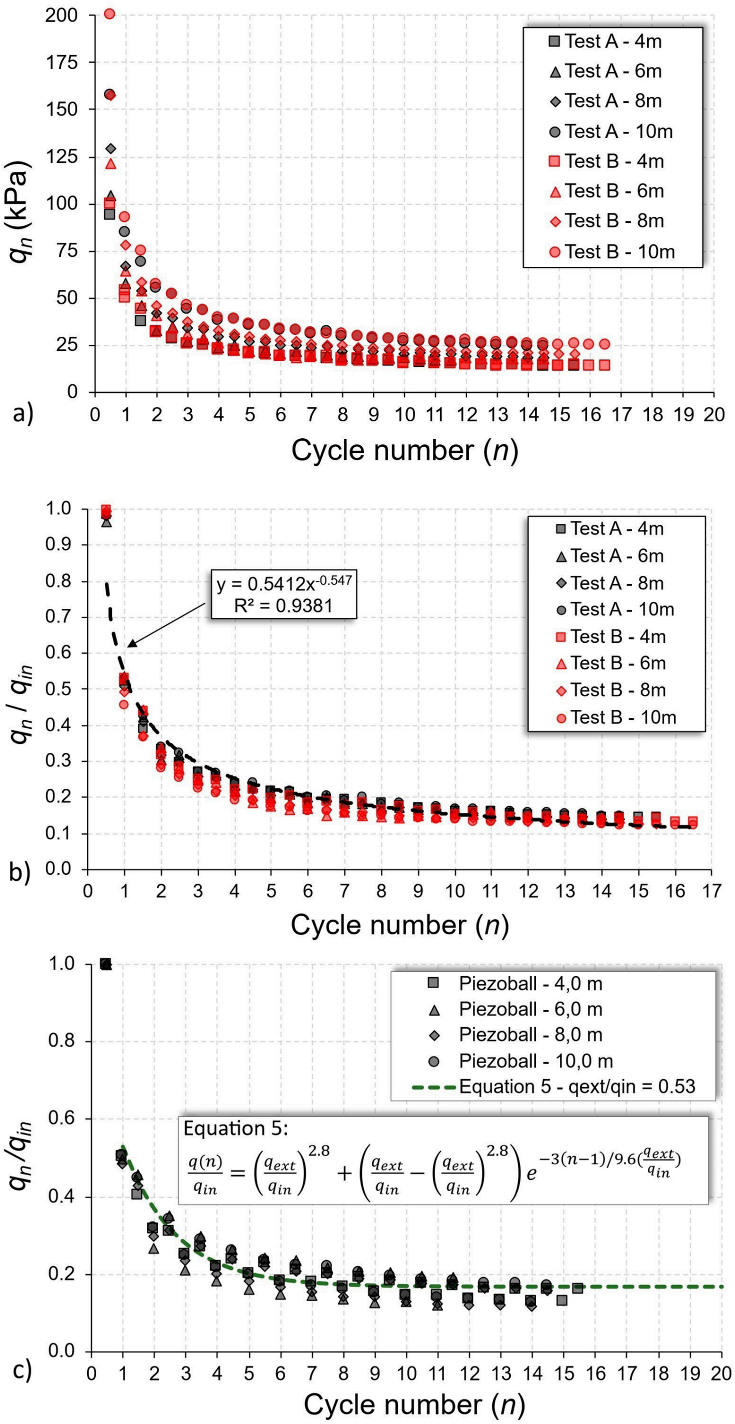

Figure 6. Cycling test analysis (a) q_n (b) normalized degradation curve – q_n/q_{in} (c) normalized degradation curve q_n/q_{in} and prediction considering Equation 5.

Equation 11 under Hypothesis ii, the resulting N_b values closely match those obtained from FVT up to a depth of 7 m. Below this depth, a greater dispersion is observed, although the mean remains consistent at 12.21. Similarly, values calculated using Hypothesis iii yield a comparable average N_b of 12.61. The greatest variability was observed for Hypothesis i, based on Test A. A similar trend is seen for N_{rem}, with mean values of 13.61 from FVT, 15.07 from Hypothesis ii (total extraction), 14.42 from Hypothesis iii, and 19.88 from Hypothesis i, Test A.

Using the average N_b value of 12.98, Figure 7 presents the undrained shear strength (S_u) estimated from piezoball tests

Table 4. Summary of S_T, N_b and N_{rem} determination.

Depth (m)	FVT			Piezoball Test A						Piezoball Test B					
				Hypothesis i			Hypothesis ii			Hypothesis iii BD			Hypothesis iv AD		
	S_T	N_b	N_{rem}	S_T	N_b	N_{rem}	S_T	N_b	N_{rem}	S_T	N_b	N_{rem}	S_T	N_b	N_{rem}
-2.0	2.8	13.0	13.5				3.9	13.2	13.3						
-3.0	1.8	13.2	13.3				3.5	13.2	13.2						
-4.0	1.8	13.2	13.3	12.6	8.0	19.7		13.2	13.3	2.8	9.6	18.7	10.6	13.2	13.2
-5.0	2.7	13.1	13.4				3.9	13.2	13.3						
-6.0	2.9	13.0	13.6	13.0	7.7	19.9		12.8	14.2	3.2	10.0	18.4	10.2	13.2	13.2
-7.0	3.2	13.0	13.6				9.0	11.1	17.2						
-8.0	4.2	12.7	14.1	14.4	7.0	20.2		13.1	13.4	6.1	6.9	20.2	14.6	12.9	14.1
-9.0	3.8	12.8	13.9				10.0	10.2	18.2						
-10.0	3.5	12.9	13.8	12.4	8.1	19.7		9.9	19.6	9.0	6.0	20.6	19.7	11.2	17.1
Average	2.9	13.0	13.6	13.1	7.7	19.9	6.1	12.2	15.1	5.3	8.1	19.5	13. 8	12.6	14.4

Table 5. Summary of dissipation tests.

Depth (m)	c_h (cm²/s)					
	Teh & Houlsby (1991)	Mahmoodzadeh et al. (2015)		Colreavy et al. (2016)		Liu et al. (2023)
	u_2	u_2	u_3	u_2	u_3	u_3
6	9.99E-03	4.77E-03	4.62E-03	6.12E-03	3.62E-03	7.53E-03
8	5.89E-03	6.78E-03	3.73E-03	9.33E-03	4.13E-03	6.08E-03
10	-	1.23E-02	4.34E-03	1.92E-02	5.32E-03	7.07E-03

A and B along depth, alongside the results from piezocone and vane tests. The S_u values range from approximately 3.0 to 13 kPa, showing a general increase with depth.

Similarly, adopting an average N_{rem} value of 13.6, Figure 7d shows the remolded undrained shear strength (S_{ur}) derived from piezoball tests A and B. The S_{ur} values estimated from the cycling stages of tests A and B range from 1.0 to 1.8 kPa and are consistent between the two tests, reflecting the similar magnitudes of q_{rem} observed. The predictive model by Yafrate et al. (2009) (Equation 13) resulted in slightly increasing S_{ur} values with depth, from approximately 1.0 to 3.0 kPa, closely matching the vane test results.

Dissipation tests were performed in Test B at depths of 6, 8, and 10 m. Table 5 summarizes the interpreted values of c_h according Teh & Houlsby (1991) solution for piezocone tests; Mahmoodzadeh et al. (2015) and Colreavy et al. (2016) for piezoball tests at positions u_2 and u_3; and Liu et al. (2023) for the piezoball at position u_3 (Equations 16, 19, 21, and 20, respectively). Device diameters were considered for calculating T. Additionally, theoretical curves by Teh & Houlsby (1991) were plotted for the u_1 and u_2 positions of the piezocone. The rigidity index I_r used was 108, as derived from triaxial test data following the approach by Schnaid et al. (1997), in which the rigidity index is defined as the ratio between the undrained shear strength (S_u) and the secant elastic modulus (E) evaluated at 50% strain.

Overall, as shown in Figure 8, dissipation curves exhibit a similar monotonic (contractive) behavior across the different test configurations. Notably, the measurements at the equator position (u_3) of the piezoball are the closest to those obtained from the piezocone tests. In contrast, at a depth of 6 m, the theoretical curve for u_1 in the piezocone shows good agreement with the piezoball readings at the middle face position (u_2). This similarity may be attributed to the analogous migration mechanisms of compressive and shear stresses around the probe in these sensor locations across the two penetrometers. In general, the coefficient of consolidation estimated by different methodologies had a magnitude around 10^{-3} cm²/s. The best approximation between estimated values considering piezocone and piezoball test was obtained by Liu et al. (2023) application.

5. Discussion and concluding remarks

The results presented in this study highlight several key aspects regarding the application of the piezoball penetrometer in a Brazilian soft soil deposit. Good repeatability was observed between the two tests (A and B), especially in the evaluation of undrained strength and remolded resistance. The undrained shear strength values obtained along the depth ranged from 3 to 13 kPa, derived using N_b values of 12.98, which is consistent with the range reported in the literature.

The strength degradation behavior obtained from cyclic tests showed stabilization of the degradation ratio (q_n/q_{in}) at approximately 0.15 after about ten cycles. The stabilized penetration resistance (q_n) was used to calculate the remolded undrained shear strength (S_{urem}). In this context,

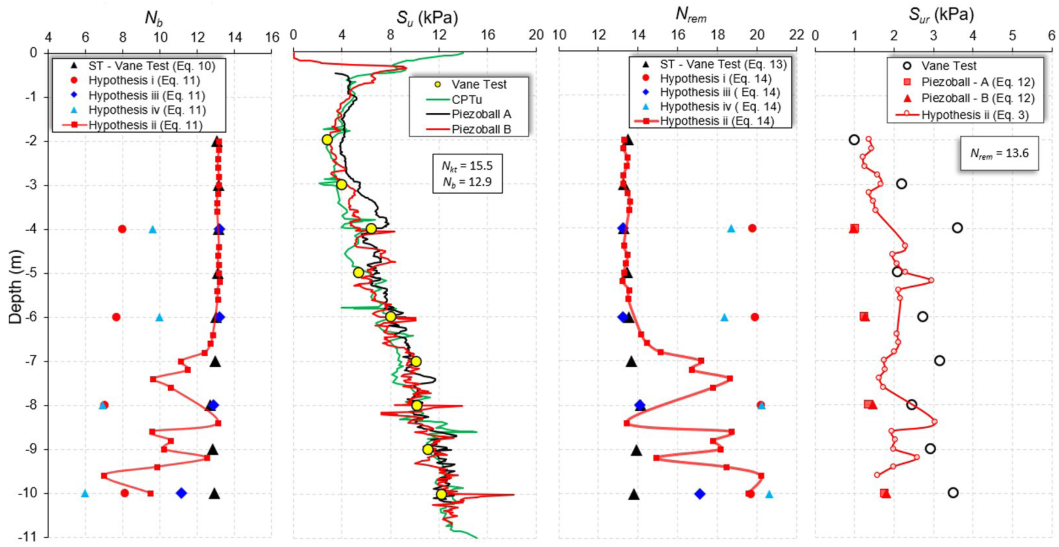

(a) (b) (c) (d)

Figure 7. Undrained strength evaluation (a) strength factor, N_b; (b) shear strength S_u; (c) remolded strength factor, N_{rem} and (d) remolded shear strength S_{ur}.

different approaches for estimating the remolded bearing factor (N_{b_rem}) were evaluated. The best agreement was obtained when N_{b_rem} was derived from field vane test results. In contrast, the method proposed by Yafrate et al. (2009) did not yield satisfactory results, particularly in cases with longer time intervals between penetration (q_{in}) and extraction (q_{ext}) readings. Longer intervals led to deviations in the estimation of q_{rem} due to partial reconsolidation or thixotropic effects, potentially resulting in an overestimation of strength recovery. These findings emphasize the importance of performing cyclic and extraction tests with minimal delay between readings or adopting monotonic procedures without prior dissipation. Nevertheless, any modifications to testing protocols should be carefully evaluated.

In terms of pore pressure dissipation analysis, the results demonstrated that appropriate interpretation depends on both the sensor position and the theoretical model adopted. Among the evaluated approaches, Liu et al.'s (2023) normalization provided better consistency between piezoball and piezocone data, especially when using sensor u_3. This suggests that the stress distribution and drainage pathways in the soil during testing may be more compatible with this model. The consolidation coefficients obtained for the deposit were on the order of approximately 7x10^{-3} cm^2/s.

5.1 Limitations and future work

With the aim of supporting future applications, this section summarizes the main limitations and practical difficulties identified during the development of this research. It also briefly outlines the sequence of studies that can be performed to address these issues in subsequent works.

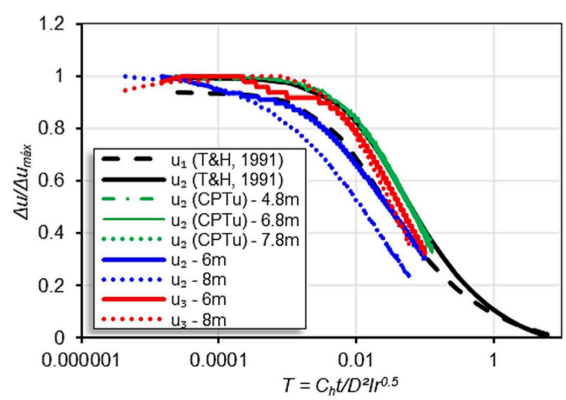

Figure 8. Excess pore pressure normalized *versus* time factor: Teh & Houlsby (1991) proposal.

Observed issues and practical challenges for future work:

- Saturation and clogging of porous elements: Difficulties were encountered in maintaining saturation of the porous stones, and clogging sometimes led to abrupt loss of pore pressure readings. The porous elements used were custom-made and have dimensions significantly smaller than those typically employed in piezocone tests, making them more sensitive to these issues. As a result, several readings were lost, and subsequent adaptations were made to the sensor positioning. The results presented in this paper predate these modifications; therefore, they are not discussed here and will be the focus of future works.
- Interpretation methods, particularly those based on sensitivity (S_T): Existing interpretation approaches

did not prove to be fully adequate or require adjustments. In particular, the determination of S_T from extraction data was not found to be reliable. A likely explanation is associated with the specific characteristics of the local soils, which differ from those where the original methods were developed. This reinforces the importance of site-specific studies and local calibration. Future work will present results from complementary testing campaigns conducted in Tubarão/SC and Sarapuí/RJ, which are currently under discussion.

- Execution of dissipation tests: Although robust theoretical frameworks exist for interpreting dissipation tests, important gaps remain. There is no clear guidance regarding the combined execution of cyclic loading and dissipation tests within the same penetration profile. From a practical standpoint, the ability to obtain both sensitivity and consolidation parameters (e.g., c_h) from a single vertical sounding would be highly advantageous. However, the allowable tolerance and potential interference between these procedures remain unclear. The literature recommends initiating cyclic loading immediately after penetration (DeJong et al., 2011), whereas O'Loughlin et al. (2020) emphasize the importance of local variations that may better represent real engineering problems. Accordingly, those authors propose the use of episodic cyclic tests emphasizing that protocols of interpretation should be adapted to site-specific conditions.

Acknowledgements

This paper was carried out with the support of the Santa Catarina Research Foundation (FAPESC) and National Council for Scientific and Technological Development (CNPq). The authors also thank the Soil Mechanics Lab and the Postgraduate Program in Civil Engineering (PPGEC) of the Federal University of Santa Catarina (UFSC) and Geoforma Engenharia for their assistance in the elaboration of this study.

Declaration of interest

The authors have no conflicts of interest to declare. All coauthors have observed and affirmed the contents of the paper, and there is no financial interest to report.

Authors' contributions

Jonatas Sosnoski: Conceptualization, Data curation, Formal analysis, Investigation, Methodology, Visualization, Writing – original draft. Gracieli Dienstmann: Conceptualization, Resources, Supervision, Writing – review & editing. André Luis Meier: Data curation, Formal analysis, Visualization, Writing – review & editing. Edgar Odebrecht: Conceptualization, Resources, Supervision, Writing – review & editing. Helena Paula Nierwinski: Writing – review & editing.

Data availability

The datasets generated during and/or analyzed during the current study are available from the corresponding author on reasonable request.

Declaration of use of generative artificial intelligence

This work was prepared without the assistance of any generative artificial intelligence (GenAI) tools or services. All aspects of the manuscript were developed solely by the authors, who take full responsibility for the content of this publication.

List of symbols and abbreviations

a	Load cell area ratio
c'	Effective cohesion
c_h	Horizontal consolidation parameter
c_v	Vertical consolidation parameter
d	Pushing rod diameter
e_0	Initial void ratio
n	Number of cycles
q_{ext}	Extraction resistance
q_{in}	Penetration resistance
q_m	Piezoball penetration resistance
q_n	Resistance of a given cycle
q_{net}	Net penetration resistance
q_{rem}	Remolded penetration resistance
q_t	Tip penetration resistance
t	Time
t_{50}	Time required for 50% excess pore pressure dissipation
t_{max}	Maximum excess pore pressure's time
u	Hydrostatic pore pressure
u_1	Probe's tip pore pressure
u_2	Probe's mid face pore pressure
u_3	Probe's equator pore pressure
w	Water content
A_p	Cross-sectional area of the probe
A_R	Area ratio
A_s	Cross-section area of the pushing rod
C_c	Compressibility coefficient
C_r	Recompression coefficient
D	Probe diameter
D_b	Piezoball diameter
D_c	Piezocone diameter
G	Particle density
IC_{RW}	Soil index
IP	Plasticity index

Ir Rigidity index
LL Liquid limit
LP Plastic limit
N_{95} Number of cycles for ninety-five percent degradation
N_b Piezoball shear strength factor
N_{kt} Piezocone shear strength factor
N_{rem} Remolded shear strength factor
N_t Piezo-T shear strength factor
OCR Over consolidation ratio
S_T Sensitivity
S_u Undrained shear strength
S_{ur} Remolded undrained shear strength
T Time factor
T_{50} Time factor required for 50% excess pore pressure dissipation
T_b Piezoball time factor
T_{b50} Piezoball time factor required for 50% excess pore pressure dissipation
USCS Universal soil classification system
α Roughness factor
σ Normal stress
σ_c Confining stress
σ_{v0} Total overburden stress
σ'_{v0} Effective overburden stress
γ Specific soil weight
Δt Time gap between measurements
Δu Excess pore pressure
Δu_{ini} Initial excess pore pressure
φ' Effective friction angle

References

ASTM D5778 (2020). *Standard test method for electronic friction cone and piezocone penetration testing of Soils*. ASTM International, West Conshohocken, PA.

Baroni, M. (2010). *Geotechnical investigation of highly compressible organic clays in deposits in Barra da Tijuca* [Master's dissertation]. Federal University of Rio de Janeiro (in Portuguese).

Chen, B.S., & Mayne, P.W. (1996). Statistical relationships between piezocone measurements and stress history of clays. *Canadian Geotechnical Journal*, 33(3), 488-498. http://dx.doi.org/10.1139/t96-070.

Chung, S.F., & Randolph, M.F. (2004). Penetration resistance in soft clay for different shaped penetrometers. In A.V. Fonseca, & P.W. Mayne (Eds.), *2nd international conference on geotechnical and geophysical site characterization* (pp. 671–677), Rotterdam: Millpress.

Colreavy, C., O'Loughlin, C.D., Long, M., Boylan, N., & Ward, D. (2010). Field experience of the piezoball in soft clay. In *2nd international symposium on cone penetration testing*, Huntington Beach, USA

Colreavy, C., O'Loughlin, C.D., & Ward, D. (2012). Piezoball testing in soft lake sediments. In R.Q. Coutinho, & P.W. Mayne (Eds.), *4th international conference on geotechnical and geophysical site characterization* (pp. 597-602). London: Taylor & Francis.

Colreavy, C., O'Loughlin, C.D., & Randolph, M.F. (2015). Experience with a dual pore pressure element piezoball. *Int J Phys Modelling Geotech*, 16(3), 101-118. http://dx.doi.org/10.1680/jphmg.15.00011.

Colreavy, C., O'Loughlin, C.D., & Randolph, M.F. (2016). Estimating consolidation parameters from field piezoball tests. *Geotechnique*, 66(4), 333-343. http://dx.doi.org/10.1680/jgeot.15.P.106.

Coutinho, R.Q. (2007). Characterization and engineering properties of Recife soft clays – Brazil. In T.S. Tan, K.K. Phoon, D.W. Hight, & S. Leroueil (Eds.), *Characterization and engineering properties of natural soils*. Boca Raton: CRC Press.

DeJong, J.T., Yafrate, N.J., & Randolph, M.F. (2008). Use of pore pressure measurements in a ball full-flow penetrometer. In A.B. Huang, & P.W. Mayne (Eds.), *3rd Int Conf on Geotechnical and Geophysical Site Characterization* (pp. 1269–1275), London: Taylor & Francis.

DeJong, J.T., Yafrate, N.J., DeGroot, D.J., Low, H.E., & Randolph, M.F. (2010). Recommended practice for full-flow penetrometer testing and analysis. *Geotechnical Testing Journal*, 33(2), 137-149. http://dx.doi.org/10.1520/GTJ102468.

DeJong, J.T., Yafrate, N.J., & DeGroot, D.J. (2011). Evaluation of undrained shear strength using full-flow penetrometers. *Journal of Geotechnical and Geoenvironmental Engineering*, 137, 14-26. http://dx.doi.org/10.1061/(ASCE)GT.1943-5606.0000393.

Dienstmann, G., Cordeiro, R.F., & Sakamoto, M.Y. (2021). Compressibility and stability analysis of an embankment on soft soil: a case study. *Proceedings of the Institution of Civil Engineers -. Geotechnical Engineering*, 175(6), 570-591. http://dx.doi.org/10.1680/jgeen.20.00140.

Einav, I., & Randolph, M.F. (2005). Combining upper bound and strain path method for evaluating penetration resistance. *J. Numer. Methods Eng*, 63(14), 1991-2016. http://dx.doi.org/10.1002/nme.1350.

ISO 19901-8:2023 (2023). *Oil and gas industries including lower carbon energy — Offshore structures — Part 8: Marine soil investigations*. International Organization for Standardization, Geneva.

Kelleher, P.J., & Randolph, M.F. (2005). Seabed geotechnical characterization with a ball penetrometer deployed from the portable remotely operated drill. In S. Gourvenec, & M. Cassidy (Eds.), *Frontiers in offshore geotechnics*. London: Taylor & Francis. p. 365–371. https://doi.org/10.1201/NOE0415390637.CH35

Liu, K., Wang, D., & Zheng, J. (2023). Numerical study of piezoball dissipation test with penetration under partially drained conditions. *Computers and Geotechnics*, 159, 105469. http://dx.doi.org/10.1016/j.compgeo.2023.105469.

Low, H.E., Randolph, M.F., & Kelleher, P.J. (2007). Comparison of pore pressure generation and dissipation rates from cone and ball penetrometers. *In: 6th International Conference on Offshore Site Investigation and Geotechnics: Confronting New Challenges and Sharing Knowledge* (pp. 547–556), London: Society for Underwater Technology.

Lunne, T., Andersen, K.H., Low, H.E., Randolph, M.F., & Sjursen, M. (2011). Guidelines for offshore in situ testing and interpretation in deepwater soft clays. *Canadian Geotechnical Journal*, 48(4), 543-556. http://dx.doi.org/10.1139/t10-088.

Lunne, T., Berre, T., & Strandvik, S. (1997). Sample disturbance effects in soft low plastic Norwegian clay. In *Proceedings of the Symposium on Recent Developments in Soil and Pavement Mechanics*, Rio de Janeiro.

Mahmoodzadeh, H., & Randolph, M.F. (2014). Penetrometer testing - the effect of partial consolidation on subsequent dissipation response. *Journal of Geotechnical and Geoenvironmental Engineering*, 140(6), 04014022. http://dx.doi.org/10.1061/(ASCE)GT.1943-5606.00011.

Mahmoodzadeh, H., Wang, D., & Randolph, M.F. (2015). Interpretation of piezoball dissipation testing in clay. *Geotechnique*, 65(10), 831-842. http://dx.doi.org/10.1680/jgeot.14.P.213.

Mayne, P.W. (2007). *Cone penetration testing: a synthesis of highway practice* (NCHRP Synthesis, No. 368). Washington, DC: National Cooperative Highway Research Program.

Meert, R. (2022) *Desenvolvimento, execução e validação dos ensaios de barra e bola* [Master's dissertation]. Universidade do Estado de Santa Catarina.

Odebrecht, E., & Schnaid, F. (2018). Assessment of the stress history of quaternary clay from Piezocone tests. *Soils and Rocks*, 41(2), 179-189. http://dx.doi.org/10.28927/SR.412179.

O'Loughlin, C., White, D., Randolph, M., Zhou, Z., & Stanier, S. (2020). Advances in full flow penetrometer testing. In T. Huszák, A. Mahler, & E. Koch (Eds.), In *6th International Conference on Geotechnical and Geophysical Site Characterization*. London: International Society for Soil Mechanics and Geotechnical Engineering. Retrieved in June 1, 2025, from https://www.issmge.org/uploads/publications/25/111/ISC2020-497.pdf

Qiao, H., Liu, L., He, H., Liu, X., Liu, X., & Peng, P. (2023). The practice and development of t-bar penetrometer tests in offshore engineering investigation: a comprehensive review. *Journal of Marine Science and Engineering*, 11, 1160. http://dx.doi.org/10.3390/jmse11061160.

Randolph, M., Hefer, P., Geise, J., & Watson, P. (1998). Improved seabed strength profiling using T-bar penetrometer. In *Proceedings of the Offshore Site Investigation and Foundation Behaviour: New Frontiers—Proceedings of an International Conference*, London, UK, 22–24 September 1998.

Randolph, M.F. (2004). Characterization of soft sediments for offshore applications. In *2nd International Conference on Site Characterization* (pp. 209-232), Porto, Portugal.

Robertson, P.K. (2009). Interpretation of cone penetration tests: a unified approach. *Canadian Geotechnical Journal*, 46(11), 1337-1355. http://dx.doi.org/10.1139/T09-065.

Robertson, P.K., & Wride, C.V. (1998). Evaluating cyclic liquefaction potential using the cone penetration test. *Canadian Geotechnical Journal*, 35(3), 442-459. http://dx.doi.org/10.1139/t98-017.

Schnaid, F., Sills, G.C., Soares, J.M., & Nyirenda, Z. (1997). Prediction of the coefficient of consolidation from piezocone tests. *Canadian Geotechnical Journal*, 34(2), 315-327. http://dx.doi.org/10.1139/t96-112.

Schnaid, F. (2009). *In situ testing in geomechanics*. 1st ed. London: Taylor & Francis Group. 330 p.

Sosnoski, J. (2024). *Caracterização de solos moles através de penetrômetros de fluxo* [Doctoral thesis], Universidade Federal de Santa Catarina, 256 p.

Teh, C.I., & Houlsby, G.T. (1991). An analytical study of the cone penetration test in clay. *Geotechnique*, 41(1), 17-34. http://dx.doi.org/10.1680/geot.1991.41.1.17.

Yafrate, N.J., & DeJong, J.T. (2005). Considerations in evaluating the remoulded undrained shear strength from full-flow penetrometer cycling. In *International Symposium on Frontiers in Offshore Geotechnics (ISFOG)* (pp. 991–997). Rotterdam: Taylor and Francis.

Yafrate, N.J., & DeJong, J.T. (2007). Influence of Penetration Rate on Measured Resistance with Full Flow Penetrometers in Soft Clay. In D.J. DeGroot, C.V. Vipulanandan, J.A. Yamamuro, V.N. Kaliakin, P.V. Lade, M. Zeghal, U. El Shamy, N. Lu, & C.R. Song (Eds.), *Geo-Denver - new peaks in geotechnics: advances in measurement and modeling of soil behavior (GSP 173)*. Denver: Society for Underwater Technology.

Yafrate, N.J., DeJong, J.T., DeGroot, D.J., & Randolph, M.F. (2009). Evaluation of remolded shear strength and sensitivity of soft clay using full-flow penetrometers. *Journal of Geotechnical and Geoenvironmental Engineering*, 135(9), 1179-1189. http://dx.doi.org/10.1061/(ASCE)GT.1943-5606.0000037.

Yubin, R., Yang, Q., Wang, Y., & Zhao, W. (2019). Experimental study on the undrained shear strength of deep-sea soft soil using improved T-bar penetrometer. *Marine Georesources and Geotechnology*, 38(10), 1-10. http://dx.doi.org/10.1080/1064119X.2019.1657532.